

1 **Supporting information**

2

3 17 pages, 14 Figures and 1 table

4

5 **Siderophores in cloud waters and potential impact on atmospheric**  
6 **chemistry: Photoreactivity of iron complexes under sun-simulated**  
7 **conditions**

8

9 **Monica Passananti<sup>a,b</sup>, Virginie Vinatier<sup>a,b</sup>, Anne-Marie Delort<sup>a,b</sup>, Gilles Mailhot<sup>a,b</sup>, Marcello**  
10 **Brigante<sup>a,b\*</sup>**

11 *<sup>a</sup> Université Clermont Auvergne, Université Blaise Pascal, Institut de Chimie de Clermont-Ferrand, BP 10448,*  
12 *F-63000 CLERMONT-FERRAND, FRANCE*

13 *<sup>b</sup> CNRS, UMR 6296, ICCF, F-63171 AUBIERE, FRANCE*

14

15

16 \* Corresponding author MB: University Blaise Pascal, Institute of Chemistry of Clermont-Ferrand, avenue des  
17 Landais 63171 Aubière, France; Phone +33 0473405514 e-mail: marcello.brigante@univ-bpclermont.fr

18

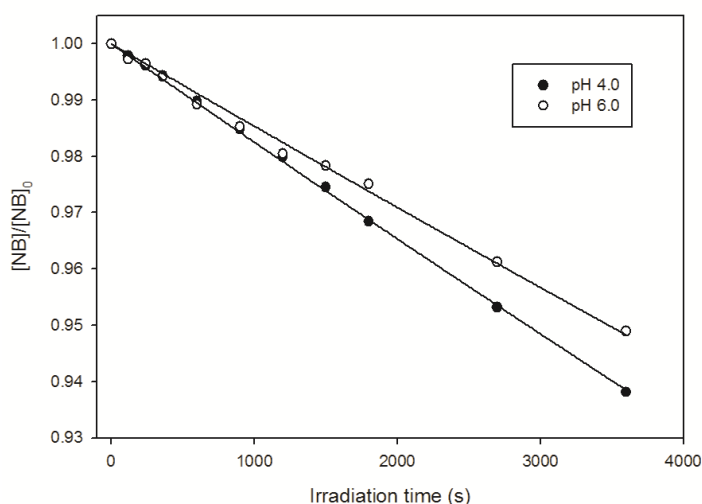
19

20 **Text S1 Nitrobenzene detection**

21 The degradation of nitrobenzene was monitored by an HPLC system (Waters Alliance)  
 22 equipped with a diode array detector (set at 210 nm) and a C18 Zorbax column (Agilent, 15  
 23 cm x 4.6 mm, 5 μm). A mixture of 50% water and 50% acetonitrile was used as the mobile  
 24 phase at a constant flow rate of 1.0 mL min<sup>-1</sup>.

25 The pseudo-first order decay of NB in the presence of 100 μM of Fe(III)-Pyo at pH 4.0 and  
 26 6.0 is showed in the following figure S1

27



28

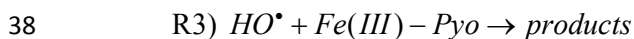
29 **Figure S1:** degradation of NB vs irradiation time in the presence of Fe(III)-Pyo 100 μM  
 30 under polychromatic irradiations

31

32 The formation rate of hydroxyl radical ( $R_{HO^\bullet}^f$ ) can be estimated using a kinetic in which  
 33 competition between NB and Fe(III)-Pyo to trap hydroxyl radical is considered:

34

35



39

40 R1 summarise the complex mechanisms discussed in the text leading to the formation of  $HO^\bullet$ ,  
 41 R2) shows the reaction between  $HO^\bullet$  and NB considering the second order rate constant  
 42 ( $k_{HO^\bullet, NB}$ ) of  $3.9 \times 10^9 M^{-1} s^{-1}$  and  $[NB] = 300 \times 10^{-6} M$ ; R3) the reactivity of  $HO^\bullet$  with Fe(III)-

43 Pyo where for  $k_{HO^\bullet, Fe(III)-Pyo}$  it is reasonable to consider the value of  $1.0 \times 10^{10} M^{-1} s^{-1}$  and  
 44  $[Fe(III)-Pyo] = 100 \times 10^{-6} M$ .

45 It is then possible to calculate the percentage of HO• trapped by NB (T<sub>HO, NB</sub>) as:

$$46 \quad T_{\text{HO, NB}} = \frac{k'_{\text{NB}}}{k'_{\text{NB}} + k'_{\text{Fe(III)-Pyo}}} \times 100 = 54\%$$

47

48 The formation rate of HO (R<sub>HO•</sub><sup>f</sup>) can be then estimated considering that 54 % of hydroxyl  
49 radical reacts with NB:

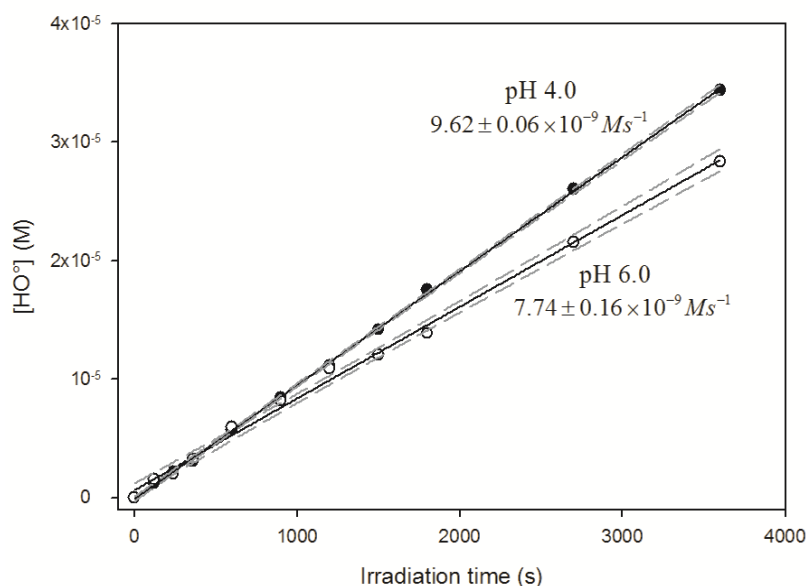
50

$$51 \quad R_{\text{HO}\cdot}^f = \frac{R_{\text{NB}}^d}{0.54}$$

52

53 R<sub>HO•</sub><sup>f</sup> vs irradiation time for pH 4.0 and 6.0 is then plotted in the Figure S2

54



55

56 **Figure S2:** Concentration of photogenerated hydroxyl radical vs irradiation time in the  
57 presence of Fe(III)-Pyo 100 μM at pH 4.0 and 6.0.

58

59

### 60 **Text S2 Formation rate and Quantum yield calculation**

61

62 The time evolution of Fe(III)-Pyo data were fitted with a pseudo-first order equation

63  $C_t = C_0 \times e^{-kt}$  where  $C_0$  and  $C_t$  are the initial concentration of Fe(III)-Pyo and concentration at  
64 time  $t$  respectively and  $k$  the first-order rate constant of Fe(III)-Pyo transformation. In this case

65 the Fe(III)-Pyo degradation rate ( $R_{\text{Fe(III)-Pyo}}^d$ ) is equal to  $k \times C_0$ .

66 The initial rates of Fe(II) formations were determined by fitting the experimental data with a

67 linear equation  $[\text{Fe(II)}] = R_{\text{Fe(II)}}^f \times t_{\text{irr}}$  considering the first 20 min of irradiation.

68 The quantum yield of photochemical reaction is defined as the ratio between molecules  
69 transformation and number of absorbed photons in the same period. This value gives an  
70 evaluation of the photochemical process efficiency independent on the experimental  
71 photochemical conditions.

72 In our experiments we assumed that Fe(III)-Pyo is the only absorbing specie present in water  
73 and the polychromatic quantum yield formation of Fe(II) ( $\phi_{Fe(II)}$ ) can be estimated in the  
74 overlap range 290-600 ( $\lambda_1$  and  $\lambda_2$ ) by (eq S1).

75

76 
$$\phi_{Fe(II)} = \frac{R_{Fe(II)}^f}{I_a} \quad \text{eq S1}$$

77 where  $R_{Fe(II)}^f$  is the Fe(II) formation rate ( $M s^{-1}$ ) and  $I_a$  is the absorbed photon flux per unit of  
78 surface and unit of time in the overlap range 290-600 ( $\lambda_1$  and  $\lambda_2$ ) by Fe(III)-Pyo. The latter  
79 was calculated from eq S2:

80

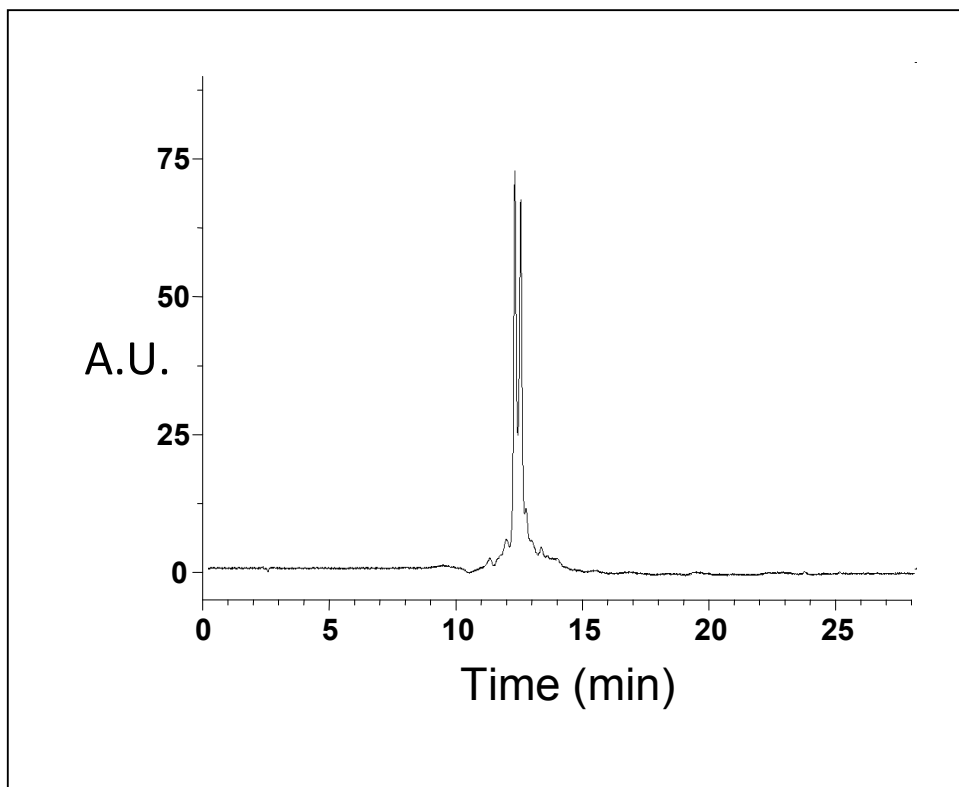
81

82 
$$I_a = \int_{\lambda_1}^{\lambda_2} I_0(\lambda) (1 - 10^{-\varepsilon(\lambda)l[Fe(III)-Pyo]}) d\lambda \quad \text{eq S2}$$

83 Where  $I_0$  is the incident photon flux,  $\varepsilon$  the molar absorption coefficient of Fe(III)-Pyo,  $l$  the  
84 optical path length inside the cells and  $[Fe(III)-Pyo]$  the initial Fe(III)-Pyo concentration.

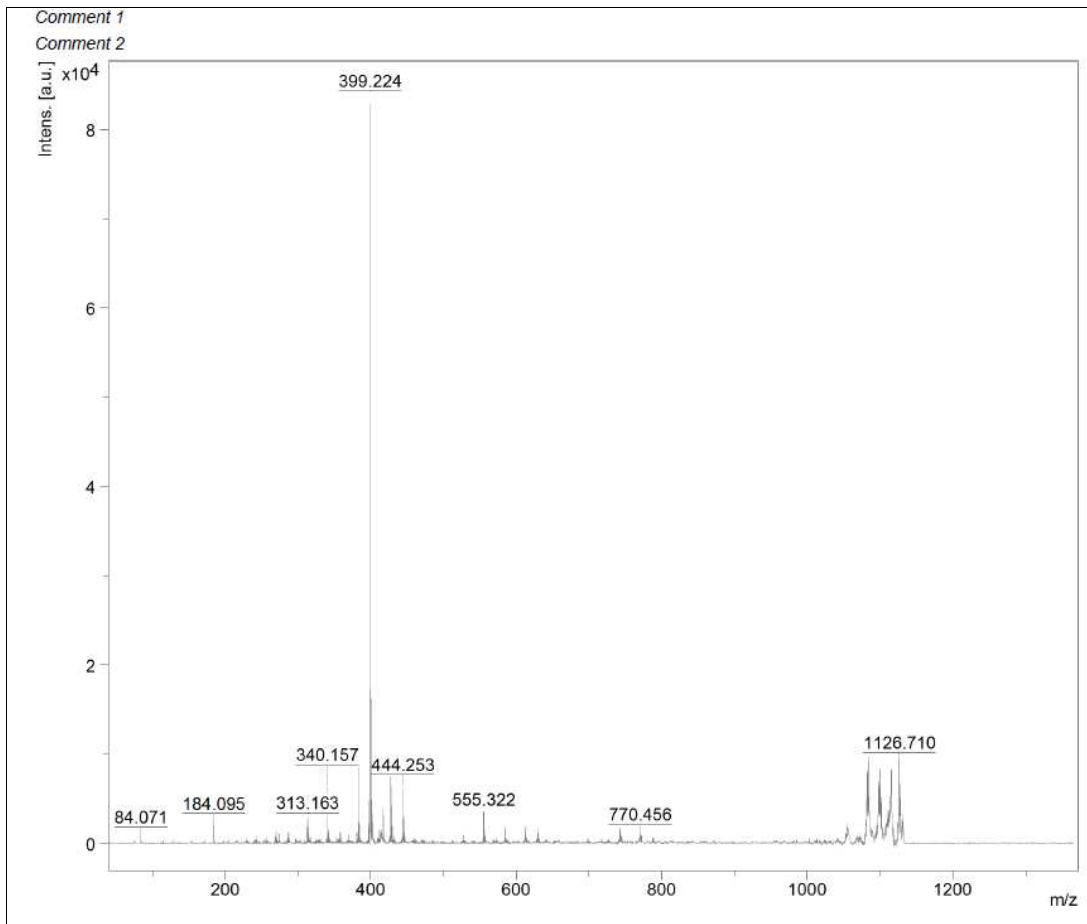
85

86



87

88 **Figure S3:** HPLC chromatogram of the purified pyoverdins obtained from *Pseudomonas*  
89 *fluorescens*36b5 culture.



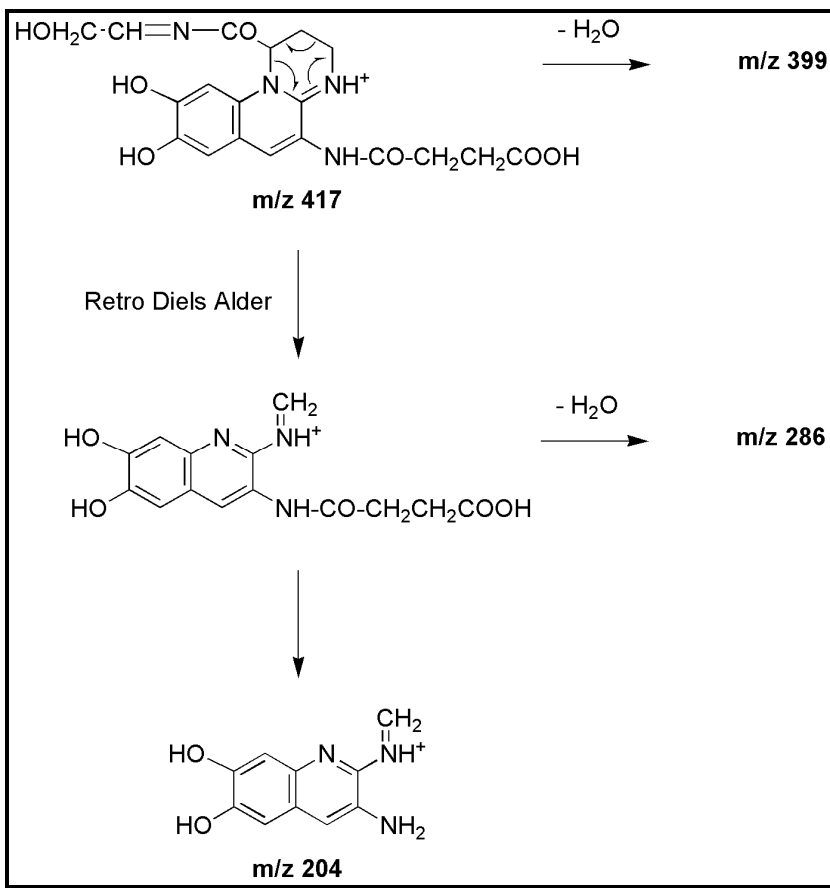
90

91 **Figure S4:** Lift (MS/MS) spectrum of the major form of pyoverdinin (m/z 1143.607).

92

m/z	Intensity	Attribution	94
84.071	1578	Lys1	
129.113	480	Lys 1	
184.095	3187	Y <sub>2</sub> -H <sub>2</sub> O-NH <sub>3</sub>	
204.104	567	Chromophore	
256.147	753	Y <sub>3</sub> -H <sub>2</sub> O-McLafferty	
274.128	1130	Y <sub>3</sub> -McLafferty	
286.143	1441	Chromophore	
313.163	3212	Y <sub>3</sub> -NH <sub>3</sub> -H <sub>2</sub> O	
399.224	84122	A <sub>1</sub> -H <sub>2</sub> O	
417.223	3942	A <sub>1</sub>	
555.322	3776	B <sub>2</sub> -H <sub>2</sub> O-CH <sub>3</sub> COOH	
770.456	1985	Y <sub>7</sub> -NH <sub>3</sub> -H <sub>2</sub> O	
1069.62	1247	[M+H] <sup>+</sup> -Mc lafferty	
1082.743	9722	[M+H] <sup>+</sup> -NH <sub>3</sub> -CO <sub>2</sub>	
1088.811	1625	[M+H] <sup>+</sup> -NOHCOCH <sub>3</sub> +H <sub>2</sub> O	
1100.902	5324	[M+H] <sup>+</sup> -NH <sub>3</sub> -CO <sub>2</sub> +H <sub>2</sub> O	
1126.71	9873	[M+H] <sup>+</sup> -NH <sub>3</sub>	

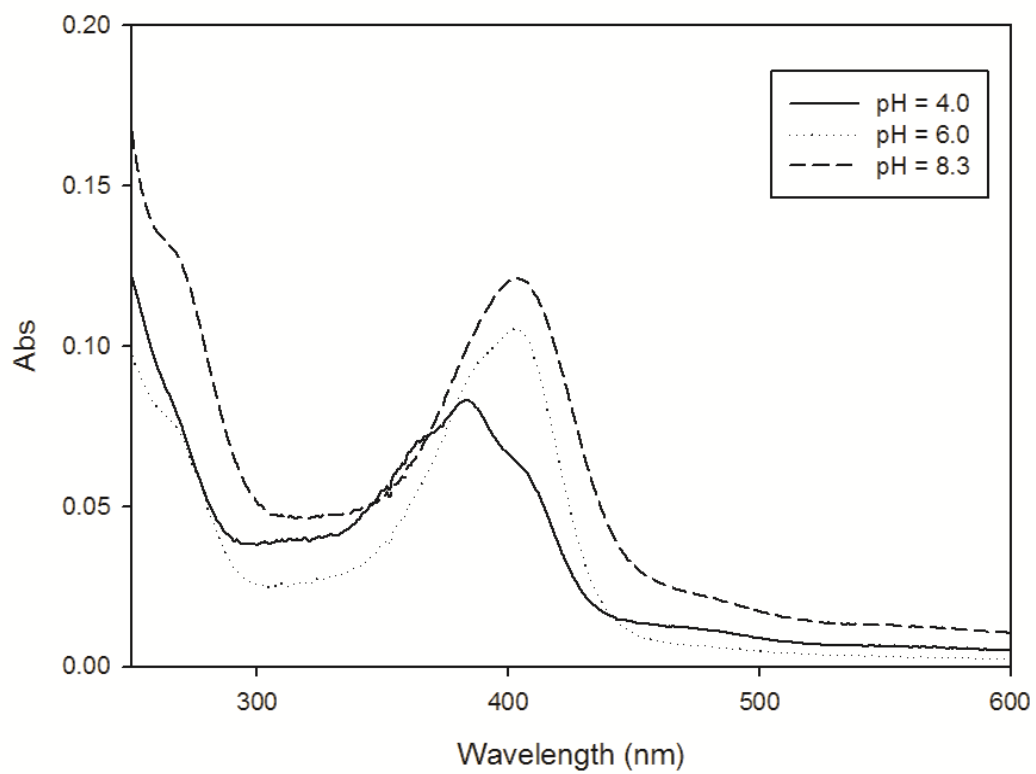
95 **Table S1:** Structure of the relevant ions obtained after fragmentation of the major form of pyoverdin  
 96 (m/z 1143.607).



97

98 **Figure S5:** MS ions obtained after fragmentation of the chromophore.

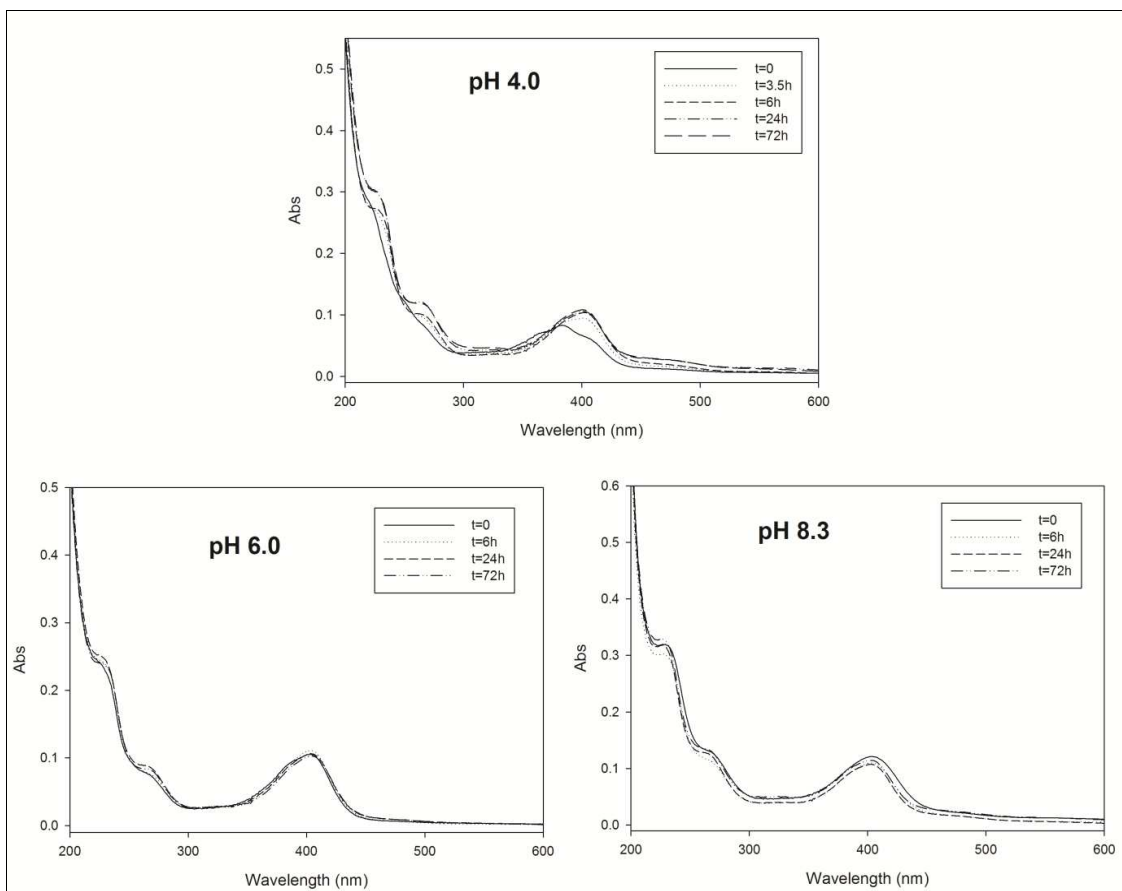
99



100

101 **Figure S6.** UV-vis absorption spectra of 100 μM pyoverdinin solution in water at pH 4.3, 6.0 and 8.3  
102 (natural pH).

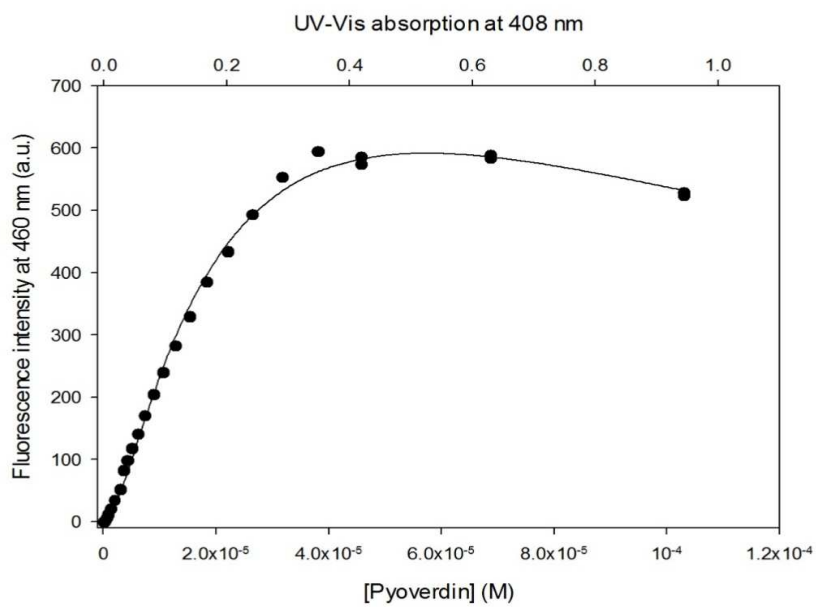
103



104

105 **Figure S7.** UV-vis evolution profile of Pyo100  $\mu\text{M}$  at pH 4.0, 6.0 and 8.3 in dark condition and 283K.

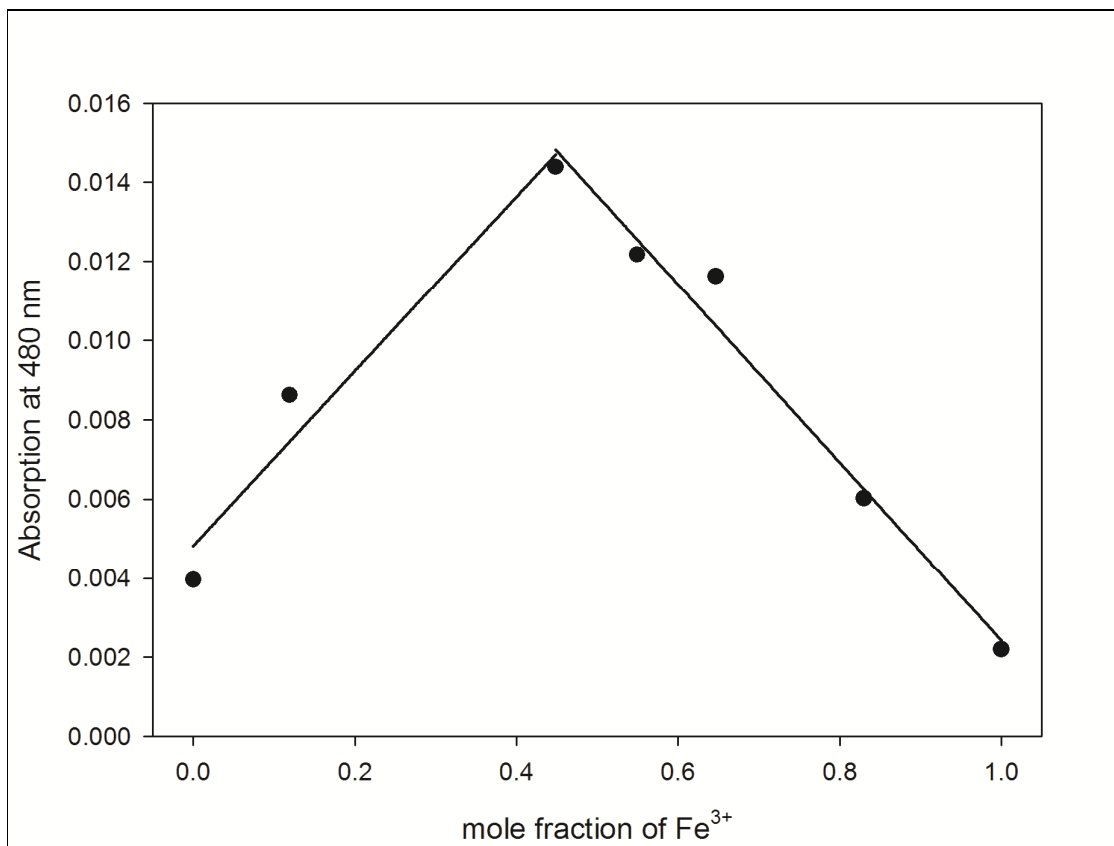
106



107

108 **Figure S8.** Correlation between pyoverdin concentration, UV-vis absorption at 408 nm (excitation  
109 wavelength) and fluorescence emission ( $\lambda_{em}$ ) intensity at 460 nm for an excitation  $\lambda_{ex} = 408$  nm.

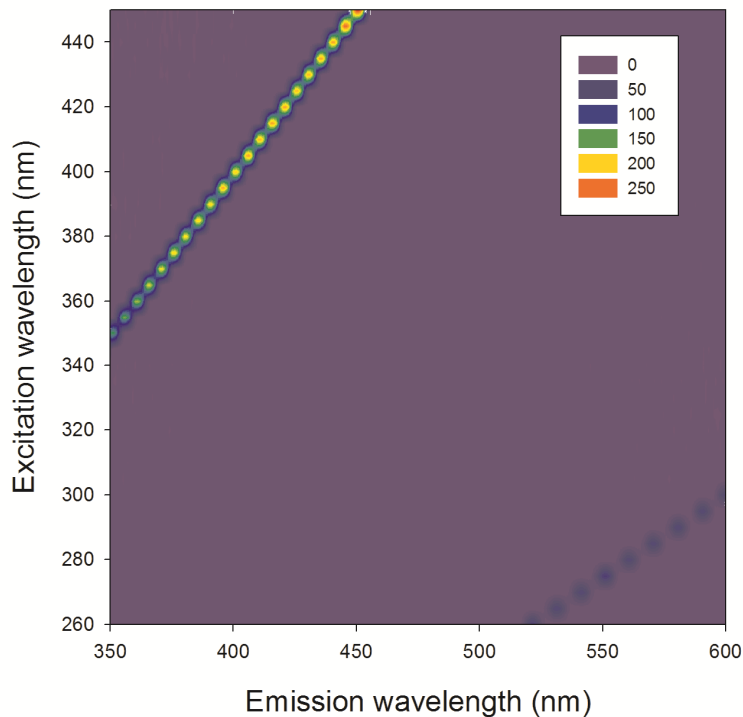
110



111

112 **Figure S9.** Assessment of Fe(III)-Pyo complex. Figure shows the standard Job's method at pH 4.0.  
113 Absorbance read at  $\lambda = 480$  nm.

114



115

116

117 **Figure S10:** Fluorescence excitation-emission matrix (EEM) as contour plot of 10 μM Fe(III)-  
 118 pyoverdine complex solution in water at pH 4.0.

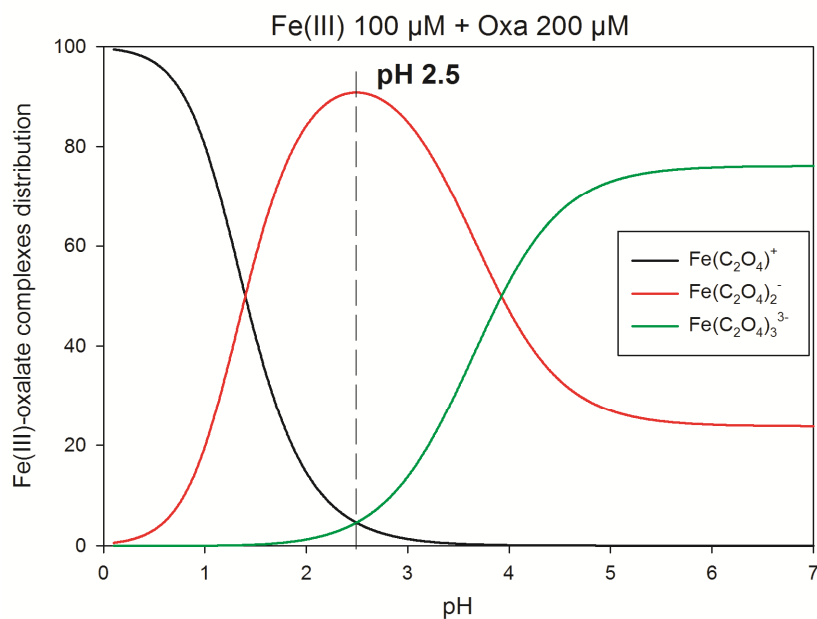
119

120

121

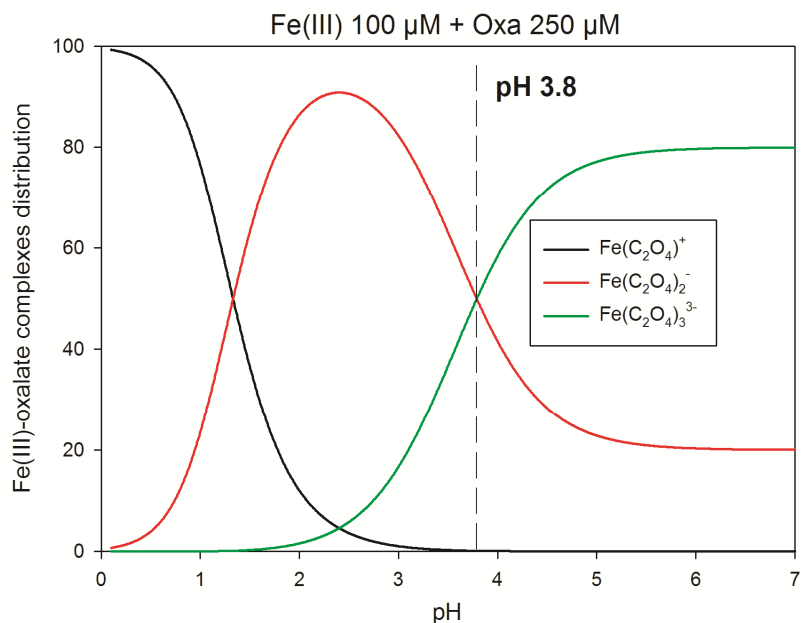
122 **Text S3 Fe-oxalate complexes**

123 The Fe(III)-oxalate complex  $\text{Fe}(\text{C}_2\text{O}_4)_2^-$  was prepared by mixing Fe(III) perchlorate (100 μM)  
 124 with potassium oxalate (200 μM) and fixing the pH at 2.5 (Figure S11). A mixture of Fe(III)-  
 125 oxalate complexes  $\text{Fe}(\text{C}_2\text{O}_4)_2^-/\text{Fe}(\text{C}_2\text{O}_4)_3^{3-}$  50/50% was prepared by mixing Fe(III)  
 126 perchlorate (100 μM) with potassium oxalate (250 μM) and fixing the pH at 3.8 (Figure S12).



127

128 **Figure S11:** Fe(III) oxalic acid complex ( $[\text{Fe(III)}] = 100 \mu\text{M}$ ,  $[\text{oxalic acid}] = 200 \mu\text{M}$ ) speciation as a  
 129 function of the pH.



130

131 **Figure S12:** Fe(III) oxalic acid complex ( $[\text{Fe(III)}] = 100 \mu\text{M}$ ,  $[\text{oxalic acid}] = 250 \mu\text{M}$ ) speciation as a  
 132 function of the pH.

133 Following parameters are used to determine iron-oxalato complexes speciation:

134 For oxalate  $K_a$  are  $5.6 \times 10^{-2}$  and  $5.42 \times 10^{-5}$  (corresponding to the first and second protonation)

135 while stability constant of Fe(III)-oxalato complexes where  $2.53 \times 10^9$ ,  $6.3 \times 10^6$ ,  $1.6 \times 10^4$

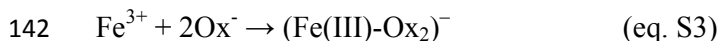
136 respectively for  $\text{Fe}(\text{C}_2\text{O}_4)^+$ ,  $\text{Fe}(\text{C}_2\text{O}_4)_2^-$  and  $\text{Fe}(\text{C}_2\text{O}_4)_3^{3-}$

137

138 **Text S4 Competition between Fe(III)-Pyo and Fe(III)-Ox<sub>2</sub> complex formation**

139 At pH 4, in the presence of oxalate (Ox) and pyoverdin (Pyo), Fe(III) can form complexes  
140 with both compounds following equations S3 and S42:

141



144

145 The corresponding stability constants are described as follow:

146  $K_{Fe(III)-Ox_2^-} = \frac{[Fe(III)-Ox_2^-]}{[Fe(III)] \times [Ox]^2} = 10^{16.2}$  (eq. S5)

147  $K_{Fe(III)-Pyo} = \frac{[Fe(III)-Pyo]}{[Fe(III)] \times [Pyo]} = 10^{20}$  (eq. S6)

148

149 where  $[Fe^{III}]$  is the free Fe(III) concentration,  $[Ox]$  is the oxalate concentration,  $[Pyo]$  is the  
150 pyoverdin concentration,  $[Fe(III)-Ox_2^-]$  is the Fe(III)-oxalate complex concentration and  
151  $[Fe(III)-Pyo]$  is the Fe(III)-Pyo complex concentration, all of these being concentrations at  
152 equilibrium.

153

154 The free Fe(III) concentration at equilibrium can be obtained by the following equation:

155

156  $[Fe(III)]_{eq} = \frac{[Fe(III)-Ox_2^-]_{eq}}{K_{Fe(III)-Ox_2^-} \times [Ox]_{eq}^2} = \frac{[Fe(III)-Pyo]_{eq}}{K_{Fe(III)-Pyo} \times [Pyo]_{eq}}$

157

158 In cloud water, the oxalate concentration is generally higher than the Fe(III) concentration.  
159 Therefore, the equilibrium concentration of free iron,  $[Fe(III)]_{eq}$  is expected to be zero. To  
160 fulfil the condition of mass balance, the sum of  $[Fe(III)-Pyo]_{eq}$  and  $[Fe(III)-Ox_2^-]_{eq}$  will  
161 be equal to the initial free Fe(III) concentration ( $[Fe(III)]_i$ ):

162  $[Fe(III)]_i = [Fe(III)-Ox_2^-]_{eq} + [Fe(III)-Pyo]_{eq}$

163 Considering the previous approximation, we can obtain the following system:

$$\begin{cases}
 [Fe(III)]_i = [Fe(III)-Ox_2^-]_{eq} + [Fe(III)-Pyo]_{eq} \\
 \frac{[Fe(III)-Ox_2^-]_{eq}}{K_{Fe(III)-Ox_2} \times [Ox]_{eq}^2} = \frac{[Fe(III)-Pyo]_{eq}}{K_{Fe(III)-Pyo} \times [Pyo]_{eq}}
 \end{cases}$$

165

166 The only unknown values are  $[Fe(III)-Pyo]_{eq}$  and  $[Fe(III)-Ox_2^-]_{eq}$ . For better, the  
 167 concentrations and the equilibrium constants are expressed as follows:

168  $[Fe(III)]_i = m$

169  $[Ox]_i = q$

170  $[Pyo]_i = n$

171  $K_{Fe(III)-Ox_2} = a$

172  $K_{Fe(III)-Pyo} = b$

173  $[Fe(III)-Ox_2^-]_{eq} = x$

174  $[Fe(III)-Pyo]_{eq} = y$

175

176 where  $[Ox]_i$  and  $[Pyo]_i$  are the initial concentration of oxalate and pyoverdin respectively.

177 The simplified systems will be:

$$\begin{cases}
 m = x + y \\
 \frac{x}{a(q-2x)^2} = \frac{y}{b(n-y)}
 \end{cases}$$

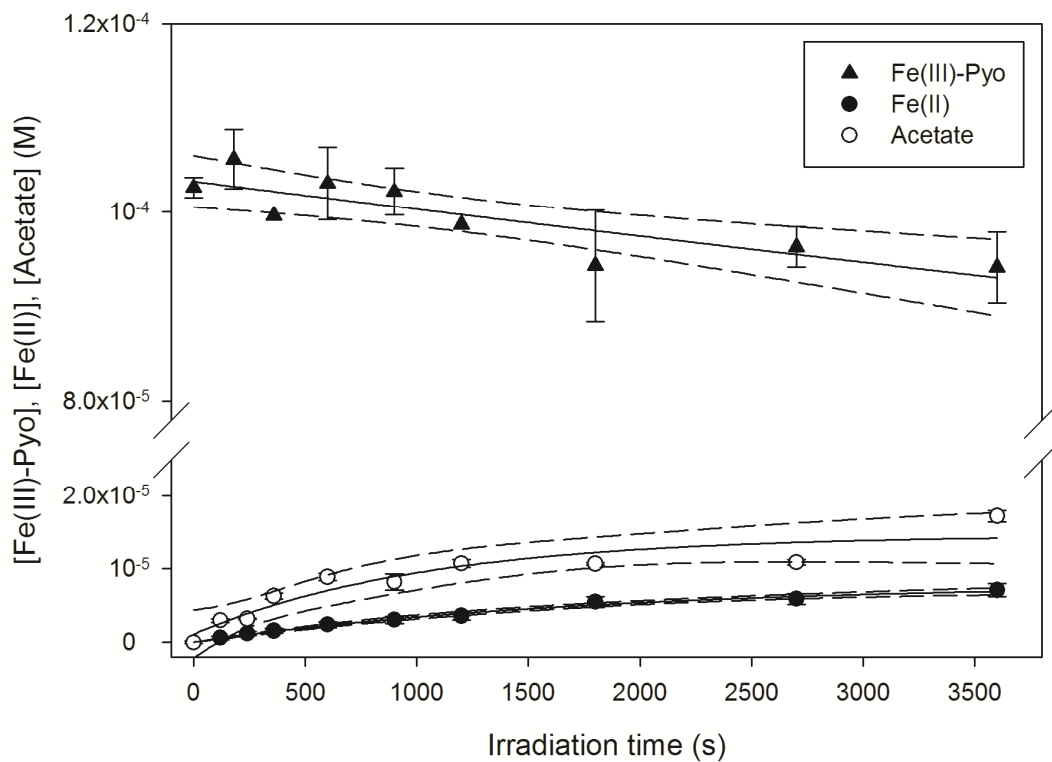
179 The solution of these simultaneous equations yields the concentrations of Fe(III)-Pyo and  
 180 Fe(III)-Ox<sub>2</sub> complexes in different conditions (different Pyo, Ox and Fe concentrations).

181

182

183

184



186

187

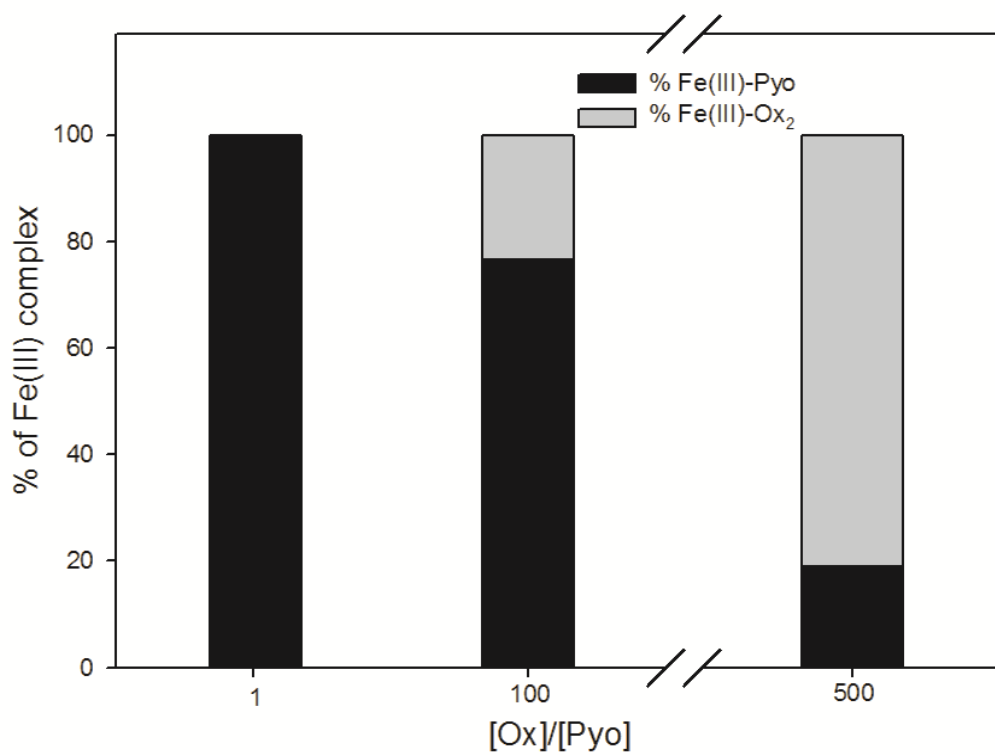
188

189

190

191

**Figure S13.** Fe(III)-Pyo degradation, Fe(II) and acetate formation profiles during polychromatic irradiation at pH 6.0. Experiments were performed at  $278 \pm 2$  K. The solid line is the fit of experimental data using an exponential decay equation for Fe(III)-Pyo and an exponential rise to a maximum value equation for Fe(II) and acetate, dashed lines denote the 95% confidence of the fit.



192  
 193  
 194  
 195  
 196  
 197

**Figure S14.** Fe(III) complex at varied Oxalate/Pyoverdine ratios ([Ox]/[Pyo]) considering an initial concentration of Fe(III) of 2 μM and Pyo of 2 μM at pH 4.0.